AMERICAN SOCIETY FOR MICROBIOLOGY | Journal of Bacteriology®

RESEARCH ARTICLE

Response Regulator CD1688 Is a Negative Modulator of Sporulation in *Clostridioides difficile*

Megan L. Kempher,[a,b] Savannah C. Morris,[a] Tyler M. Shadid,[b] Smita K. Menon,[a] Jimmy D. Ballard,[b] Ann H. West[a]

[a]University of Oklahoma, Department of Chemistry and Biochemistry, Norman, Oklahoma, USA
[b]University of Oklahoma Health Sciences Center, Department of Microbiology and Immunology, Oklahoma City, Oklahoma, USA

ABSTRACT Two-component signal transduction systems (TCSs), consisting of a sensor histidine kinase (HK) and a response regulator (RR), sense environmental stimuli and then modulate cellular responses, typically through changes in gene expression. Our previous work identified the DNA binding motif of CD1586, an RR implicated in *Clostridioides difficile* strain R20291 sporulation. To determine the role of this RR in the sporulation pathway in *C. difficile*, we generated a deletion strain of *cd1688* in the historical 630 strain, the homolog of *cd1586*. The *C. difficile* Δcd1688 strain exhibited a hypersporulation phenotype, suggesting that CD1688 negatively regulates sporulation. Complementation of the *C. difficile* Δcd1688 strain restored sporulation. In contrast, a nonphosphorylatable copy of *cd1688* did not restore sporulation to wild-type (WT) levels, indicating that CD1688 must be phosphorylated to properly modulate sporulation. Expression of the master regulator *spo0A*, the sporulation-specific sigma factors *sigF*, *sigE*, *sigG*, and *sigK*, and a signaling protein encoded by *spoIIR* was increased in the *C. difficile* Δcd1688 strain compared to WT. In line with the increased *spoIIR* expression, we detected an increase in mature SigE at an earlier time point, which arises from SpoIIR-mediated processing of pro-SigE. Taken together, our data suggest that CD1688 is a novel negative modulator of sporulation in *C. difficile* and contributes to mediating progression through the spore developmental pathway. These results add to our growing understanding of the complex regulatory events involved in *C. difficile* sporulation, insight that could be exploited for novel therapeutic development.

IMPORTANCE *Clostridioides difficile* causes severe gastrointestinal illness and is a leading cause of nosocomial infections in the United States. This pathogen produces metabolically dormant spores that are the major vehicle of transmission between hosts. The sporulation pathway involves an intricate regulatory network that controls a succession of morphological changes necessary to produce spores. The environmental signals inducing the sporulation pathway are not well understood in *C. difficile*. This work identified a response regulator, CD1688, that, when deleted, led to a hypersporulation phenotype, indicating that it typically acts to repress sporulation. Improving our understanding of the regulatory mechanisms modulating sporulation in *C. difficile* could provide novel strategies to eliminate or reduce spore production, thus decreasing transmission and disease relapse.

KEYWORDS *Clostridioides difficile*, response regulator, sporulation, two-component regulatory systems

Clostridioides difficile is a human enteropathogenic bacterium currently categorized as an urgent health care threat by the CDC due to its multidrug resistance and increasing infection rate (roughly 500,000 cases per year) (1). This bacterium is a spore-forming, obligate anaerobe that colonizes the lower gut, causing gastrointestinal symptoms ranging from diarrhea to toxic megacolon and even death (2, 3). *C. difficile* infections commonly follow antibiotic treatment, which disrupts the protective gut

Editor Tina M. Henkin, Ohio State University
Copyright © 2022 Kempher et al. This is an open-access article distributed under the terms of the Creative Commons Attribution 4.0 International license.
Address correspondence to Ann H. West, awest@ou.edu.
The authors declare no conflict of interest.

Received 6 April 2022
Accepted 30 June 2022
Published 19 July 2022

microbiota, with recurring infections happening in 15 to 35% of cases (4). Unlike vegetative cells, spores can survive aerobic conditions and are highly resistant to chemical and physical cleaning procedures, making them the primary mode of transmission between hosts (5–9).

The overall steps of spore formation involve an intricate developmental pathway that is generally conserved in members of the *Firmicutes* phylum. The first step of sporulation is asymmetric division where the cell produces a larger mother cell and a smaller forespore. Sporulation initiation is controlled by the master regulator stage 0 sporulation protein A (Spo0A) (3, 9–12), which must be phosphorylated for the pathway to be activated (10, 12–14). As a transcriptional activator, phosphorylated Spo0A (Spo0A~P) binds DNA, initiating the expression of genes necessary for the early stages of sporulation, including the cell type-specific sigma factors *sigE* and *sigF* (9, 13, 15, 16). Inactivation of Spo0A in *C. difficile* results in an asporogenic phenotype similar to what is observed in *Bacillus subtilis* (10, 17). The signal transduction pathway that controls sporulation initiation was initially and extensively studied in *B. subtilis* (15, 18, 19). However, several recent studies have revealed many key differences in the sporulation pathway of *C. difficile*. In *B. subtilis*, Spo0A phosphorylation occurs via a multistep phosphorelay system consisting of multiple sensor kinases and phosphotransfer proteins (18). In *C. difficile*, phosphorylation of Spo0A is predicted to be modulated by several orphan histidine kinases (CD1492, CD1579, CD1942, and CD2492) (10, 17). CD1492 and CD2492 repress sporulation initiation by acting as phosphatases toward phosphorylated Spo0A~P (20, 21). CD1579 has been shown to phosphorylate Spo0A *in vitro* (10), although recent studies indicate that it may also repress sporulation (21, 22).

While the specific signals initiating Spo0A phosphorylation in *C. difficile* remain unknown, several studies have demonstrated a direct link between nutrient availability and sporulation initiation. Global regulators CodY, which responds to cellular levels of branched-chain amino acids (BCAAs) and GTP (23), and CcpA, which senses global carbon availability, repress sporulation when nutrients are abundant (24). These regulators also repress expression of the *sinRR'* locus, which encodes two transcriptional regulators that are known to influence transcription of *spo0A*, and genes encoding proteins that mediate motility and toxin production (25). Recently, transcriptional regulator CD2589 was shown to decrease the abundance of *spo0A* transcripts within the cell in response to available nutrients present in the environment (26).

Two-component signal transduction systems (TCSs) are composed of a histidine kinase (HK) and a response regulator (RR) that function as a unit to sense and respond to environmental signals. HKs detect an environmental signal (nutrients, stress, antibiotics, etc.) using a sensory domain and autophosphorylate at a conserved histidine residue (27). The RR is able to induce transfer of the phosphoryl group from this phosphorylated histidine to a conserved aspartate residue in the receiver domain of the RR (28), resulting in a conformational change that alters the biological activity of the RR. The effector domain of the RR determines the biological response, the most common of which is regulation of gene expression (29). Improving our understanding of gene regulation in *C. difficile* by TCSs could reveal new targets for therapeutic development, especially since these systems are absent in animals (30).

Previously, our lab used a bacterial one-hybrid system to determine the DNA motif that RR CD1586 recognizes and binds to in the hypervirulent *C. difficile* strain R20291 (CDR20291). These analyses identified multiple putative gene targets (31). These targets included genes encoding several ion transporters, ABC transporters, enzymes involved in proteolysis, and sporulation-related proteins. RR CD1586 had been previously implicated in a transposon mutagenesis screen as being important in sporulation (32). In *C. difficile* strain 630 (CD630), the homolog to CD1586 is CD1688 (100% amino acid identity), which has a cognate HK, CD1689. Here, we report the creation of a *cd1688* deletion strain in CD630, a more genetically tractable strain than R20291, that resulted in a hypersporulation phenotype. We further show that this increased sporulation was accompanied by increased expression of sporulation-specific genes and

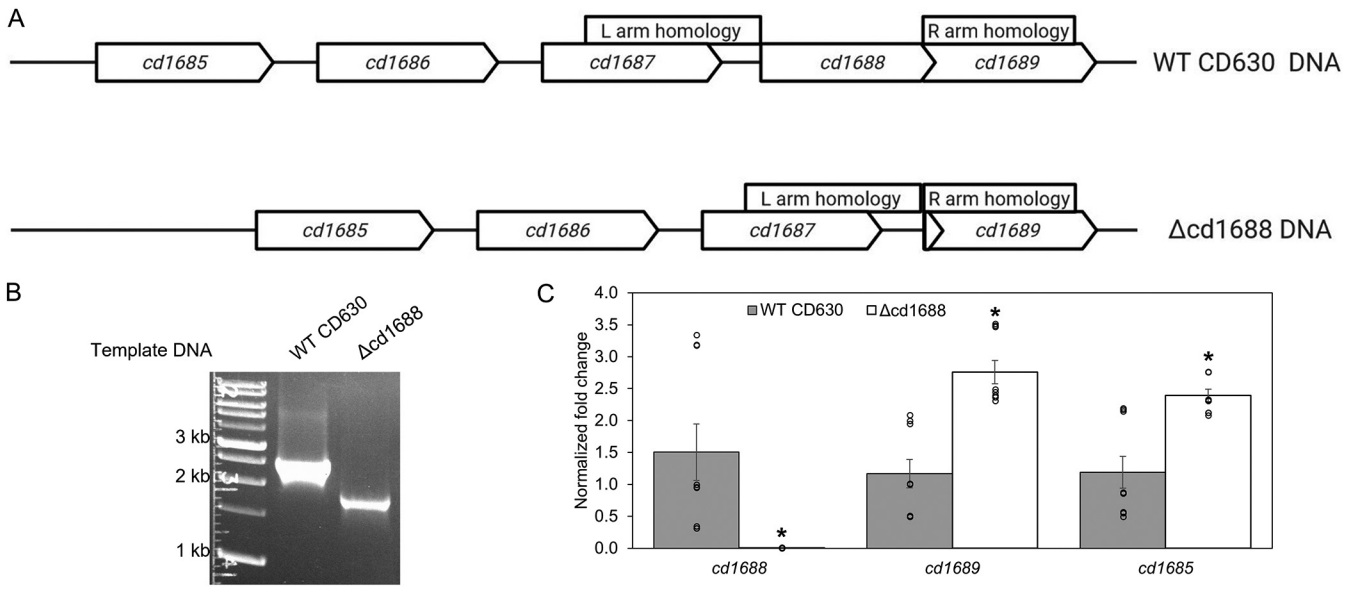

FIG 1 Deletion of the *cd1688* gene in *C. difficile*. (A) *cd1688* locus in *C. difficile* 630 wild-type (WT) and *C. difficile* Δcd1688 strains. Boxes indicate positions of homology arms used for construction of the deletion strain. (B) PCR confirmation of *cd1688* gene deletion in *C. difficile* Δcd1688. The *cd1688* gene deletion removed 661 bp. (C) Abundance of *cd1688*, *cd1689*, and *cd1685* in the *C. difficile* Δcd1688 strain relative to the WT strain measured via qRT-PCR. Three biological replicates of each strain were grown in BHIS to an OD_{600} of 1.0. *, $P \leq 0.05$.

increased processing of sporulation-specific sigma factor SigE and was dependent on phosphorylation of CD1688. Deletion of *cd1688* had no effect on the expression of toxin genes or motility. Taken together, our results demonstrate that CD1688 functions to repress sporulation in *C. difficile* under certain environmental conditions.

RESULTS

Construction of a *cd1688* deletion strain. The genes encoding RR CD1688 (*cd1688*) and HK CD1689 (*cd1689*) are located in a putative five-gene operon downstream of a hypothetical protein (*cd1685*), a transcriptional regulator (*cd1686*), and a lipoprotein (*cd1687*) (Fig. 1A). To further interrogate the role of this TCS in *C. difficile* physiology, we deleted *cd1688* in wild-type (WT) CD630 using a CRISPR-Cas9 nickase gene editing system (here named *C. difficile* Δcd1688) (see Fig. S1 in the supplemental material) (33). To confirm the desired deletion was generated, genomic DNA (gDNA) was PCR amplified using primers that flanked the expected deletion (Table S2). As shown in Fig. 1B, *C. difficile* Δcd1688 was confirmed by an expected PCR product size decrease of 2,429 bp to 1,768 bp and further verified via Sanger sequencing. We next tested the growth of the *C. difficile* Δcd1688 strain compared to WT. The *C. difficile* Δcd1688 strain grew similarly to *C. difficile* WT in brain heart infusion medium supplemented with yeast extract (BHIS) (Fig. S2), indicating that the mutation did not cause any major growth defects under standard laboratory growth conditions.

Expression of *cd1688* is likely controlled via autoregulation. As shown in Fig. 1C, as expected, *C. difficile* Δcd1688 had no detectable *cd1688* transcripts, further confirming a clean deletion. To ensure the deletion of *cd1688* did not have any polar effects on the downstream gene, we measured the expression of *cd1689*, the gene encoding the cognate HK, using quantitative reverse transcription-PCR (qRT-PCR) analysis. Expression of *cd1689* was increased ~2.8-fold in *C. difficile* Δcd1688 compared to *C. difficile* WT during stationary growth in BHIS medium (Fig. 1C). Our previous work identified a putative binding motif of CD1688 upstream of *cd1685*, the predicted operon leader of this locus. Therefore, we also measured the expression of *cd1685* in the *C. difficile* Δcd1688 strain compared to the WT strain (Fig. 1C). Expression of *cd1685* was also increased in the deletion strain (~2.1-fold). Together, these data indicate that CD1688

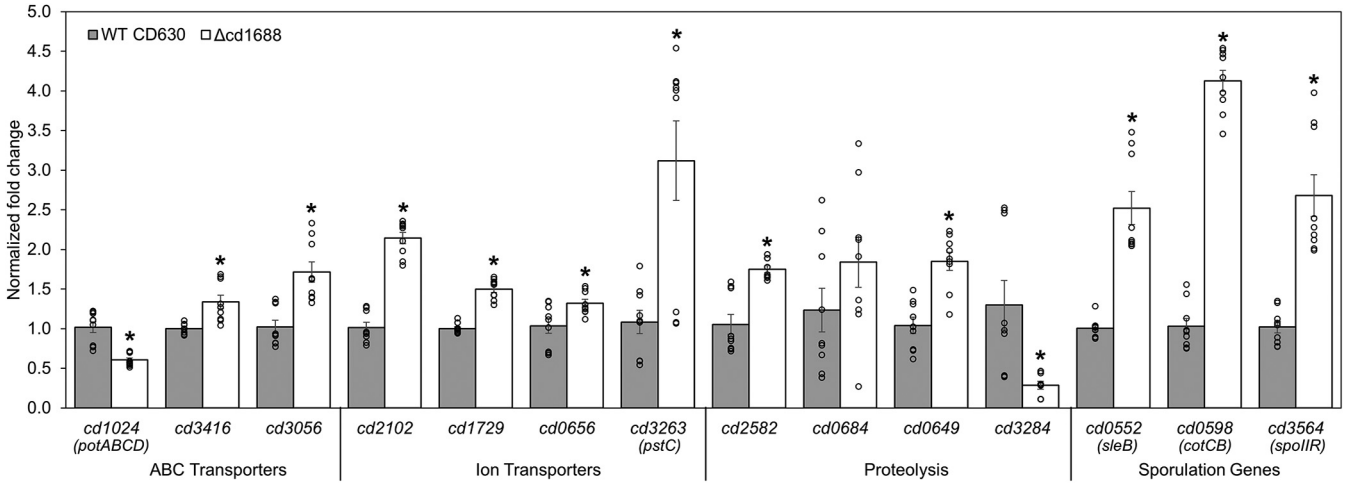

FIG 2 Transcript abundance of predicted gene targets of CD1688 in the *C. difficile* WT and Δcd1688 strains. The expression of genes involved in ABC/ion transport, proteolysis, and sporulation was measured from RNA samples isolated from three biological replicates during stationary-growth phase in BHIS medium via qRT-PCR (OD_{600}, ~1.0). The expression of each gene in the Δcd1688 strain is measured relative to the expression in the WT strain in the same growth conditions. *, $P \leq 0.05$.

likely autoregulates its own expression through regulation of the entire operon, as suggested by our previous work (31).

The expression of several predicted gene targets of CD1688 was decreased in the *C. difficile* Δcd1688 strain. We next sought to evaluate whether the expression of the predicted gene targets of CD1688, identified in our previous work (31), was affected in the *C. difficile* Δcd1688 strain versus the WT strain during growth in BHIS. The majority of the predicted targets can be categorized into one of the following functional groups: ABC/ion transport, proteolysis, or sporulation processes. Therefore, we tested the expression of the previously identified gene targets from these functional groups. All of these targets were significantly differentially expressed in the *C. difficile* Δcd1688 strain, with the exception of *cd0684* (Fig. 2). The majority of targets had increased expression in the *C. difficile* Δcd1688 strain, indicating that CD1688 likely represses these targets in the growth conditions tested. Two targets, *cd1024* and *cd3284*, which encode the *potABCD* transporter and an HtrA-like protease, respectively, showed a decrease in expression in the *C. difficile* Δcd1688 strain.

Deletion of *cd1688* increases sporulation efficiency in *C. difficile* 630 but has no effect on toxin production or motility. Since a previous transposon mutagenesis study indicated that *cd1688* was one of 798 genes likely to impact sporulation (32), we tested if deleting *cd1688* had any effect on the ability of *C. difficile* to produce spores. Phase-contrast microscopy was used to discriminate vegetative cells (phase dark) from spores (phase bright) after 24 h of growth on 70:30 sporulation plates. We saw a significant increase in the number of spores in the *C. difficile* Δcd1688 strain compared to the WT strain (Fig. 3). The sporulation efficiency was quantified by enumerating ethanol-resistant spores and vegetative cells after 24 h of growth on 70:30 sporulation plates. The *C. difficile* WT strain exhibited a sporulation efficiency of ~20%, which is similar to previously reported sporulation frequencies for WT CD630 (34) (Fig. 3A and Fig. S3). The *C. difficile* Δcd1688 strain had a sporulation efficiency of ~75%, which was ~3.75-fold higher than the WT strain (Fig. 3B and Fig. S3). These data strongly suggest that in the *C. difficile* WT strain, CD1688 acts to inhibit spore formation.

To confirm the hypersporulation phenotype was solely due to the deletion of *cd1688*, a complement strain was constructed by conjugating a vector that expresses the *cd1688* gene under a xylose-inducible promoter into the *C. difficile* Δcd1688 strain (here named *C. difficile* Δcd1688::p1688) (Fig. S4) (35). When 0.1% xylose was added to the growth medium, the sporulation efficiency of *C. difficile* Δcd1688::p1688 was restored to levels similar

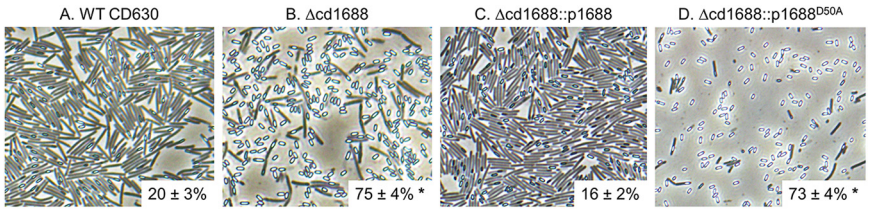

FIG 3 Sporulation efficiency of *C. difficile* WT versus Δcd1688 strains. Phase-contrast microscopy of *C. difficile* WT (A), Δcd1688 (B), Δcd1688::p1688 (C), and Δcd1688::p1688^{D50A} (D) grown on 70:30 sporulation agar supplemented with 0.1% xylose for 24 h. Inset numbers represent sporulation efficiency as measured by ethanol resistance assays. *, $P \leq 0.05$ as determined by a one-way ANOVA followed by Dunnett's multiple-comparison test compared to *C. difficile* WT630.

to *C. difficile* WT (~16%) (Fig. 3C and Fig. S3), further corroborating that the hypersporulation phenotype was due to the deletion of *cd1688*.

Since sporulation, toxin production, and motility are tightly linked via the activities of several global regulators in *C. difficile* (12, 24, 25, 36), we also tested if deleting *cd1688* had any effect on these processes. The *C. difficile* Δcd1688 strain did not show any significant changes compared to the WT strain in the expression of toxin genes *tcdA* or *tcdB* or the toxin-specific sigma factor *tcdR* (Fig. S5A), indicating that CD1688 does not appear to regulate toxin expression. We next tested motility of the *C. difficile* WT and Δcd1688 strains. Growth diameters were similar between the *C. difficile* WT and Δcd1688 strains (Fig. S5B), suggesting that CD1688 also does not affect cell motility.

Deletion of *cd1688* affects expression of other global regulators. *C. difficile* sporulation is known to be influenced by several global regulators. For example, CcpA (carbon control protein) and CodY (with cofactors BCAAs/GTP) repress sporulation when nutrient levels are high in the environment (23, 24, 37, 38). The *sin* locus encodes *sinR* and *sinR'*, which are inhibitors of sporulation in *B. subtilis* (39, 40). The mechanism of control of sporulation via SinRR' in *C. difficile* remains unclear, but studies have shown that a *sin* locus deletion was asporogenic, SinR positively regulates sporulation, and SinR' acts as an antagonist through direct binding to SinR, thus negatively influencing sporulation (25, 41). The multifunctional regulator RstA has also been shown to positively affect sporulation through a yet-to-be-identified mechanism (42, 43). To determine if any of these global regulators were differentially expressed in our *C. difficile* Δcd1688 strain, we measured transcript abundance of these genes during growth on 70:30 sporulation plates via qRT-PCR. For *ccpA*, we only observed a significant difference of expression at 10 h (1.3-fold increase) in the *C. difficile* Δcd1688 strain (Fig. 4A). Expression of *codY* was significantly different only at 12 h, with a 0.6-fold decrease in the *C. difficile* Δcd1688 strain (Fig. 4B). In contrast, both *sinR* and *sinR'* transcripts were significantly increased in the *C. difficile* Δcd1688 strain at all time points tested (Fig. 4C and D). We observed no significant changes in *rstA* expression between the *C. difficile* Δcd1688 and WT strains at any of the tested time points (Fig. 4E).

Deletion of *cd1688* results in increased expression of sporulation-specific genes. To further investigate how the deletion of *cd1688* increased sporulation efficiency, we examined the *C. difficile* Δcd1688 strain for differences in the expression of a set of genes known to be involved in initiation of sporulation. The transcript levels of *spo0A*, the master regulator of sporulation, were increased in the *C. difficile* Δcd1688 strain compared to the WT strain at 8 h (1.7-fold) and 10 h (1.3-fold) after inoculation on 70:30 sporulation agar plates but decreased compared to WT levels at 12 h (0.4-fold) (Fig. 5A). Spo0A-mediated regulation is dependent on phosphorylation and does not necessarily correlate to transcript levels (10, 44, 45). Therefore, we also measured the amount of phosphorylated Spo0A (Spo0A~P) using Phos-tag SDS-PAGE analysis from total protein harvested from the *C. difficile* Δcd1688 and WT strains at 8 h, 10 h, and 12 h postinoculation on 70:30 sporulation plates. Both unphosphorylated Spo0A and Spo0A~P forms were detected via

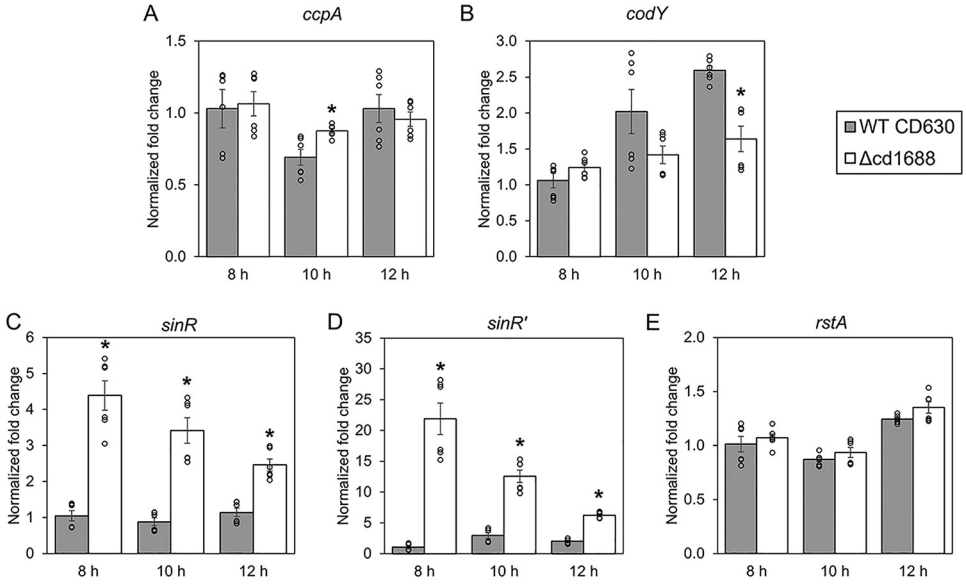

FIG 4 Transcript abundance of some known regulators of sporulation in the *C. difficile* WT and Δcd1688 strains. Expression of *ccpA* (A), *codY* (B), *sinR* (C), *sinR′* (D), and *rstA* (E) was measured from RNA samples isolated at 8 h, 10 h, and 12 h postinoculation on 70:30 sporulation media from *C. difficile* WT and Δcd1688 strains. Expression for each gene is presented relative to the WT sample at 8 h. *, $P \leq 0.05$ as determined by Student's *t* test compared to the *C. difficile* WT630 strain at the same time point.

Western blot analysis with anti-Spo0A antibody (Fig. 5B). We confirmed that the upper band corresponded to Spo0A∼P, as upon heating, this band disappeared. At the 8-h time point, the ratio of Spo0A∼P to Spo0A was higher in the *C. difficile* Δcd1688 strain than the WT strain. There was no difference between the strains at 10 h and by the 12-h time point, the ratio of Spo0A∼P to Spo0A had decreased in the *C. difficile* Δcd1688 strain compared to the WT strain.

Two well-established targets of Spo0A∼P are the cell type-specific sporulation sigma factors *sigE* and *sigF*, which control transcription of sporulation genes in the mother cell and the forespore, respectively (16). Therefore, we next measured the transcript abundance of these two genes during growth on 70:30 sporulation medium. As shown in Fig. 5C and D, *sigF* transcripts were significantly increased at 8 h (2.8-fold; see inset in Fig. 5C), while the *sigE* transcripts were significantly increased both at 8 h (4.2-fold; see inset in Fig. 5D) and 10 h (1.8-fold) in the *C. difficile* Δcd1688 strain compared to the WT strain at the same time point. The expression of genes involved in the later stages of sporulation is controlled by SigG and SigK in the forespore and mother cell, respectively. Therefore, we also measured the expression of these genes during growth on 70:30 sporulation plates. In the *C. difficile* Δcd1688 strain, *sigG* was significantly increased compared to the WT strain at the same time point for both 8-h (1.7-fold) and 10-h (1.5-fold) samples (Fig. 5E) while *sigK* was significantly increased at both 10 h (9.0-fold) and 12 h (14.5-fold) postinoculation (Fig. 5F).

CD1688 directly binds to the *spoIIR* gene promoter. Of the previously predicted gene targets of CD1688, only *spoIIR* has an identified role in regulating the sporulation pathway in *C. difficile* (46). During the spore developmental pathway, the mother cell and forespore follow distinct transcriptional programs controlled by the aforementioned cell-specific sigma factors (SigF and SigG in the forespore and SigE and SigK in the mother cell) (16). Pro-SigE must be processed into active SigE in order for the sporulation pathway to proceed in the mother cell (47, 48). Expression of *spoIIR* occurs in the forespore and is mediated by both SigF and Spo0A∼P in *C. difficile* (48). SpoIIR is secreted across the forespore inner membrane space where it interacts with SpoIIGA

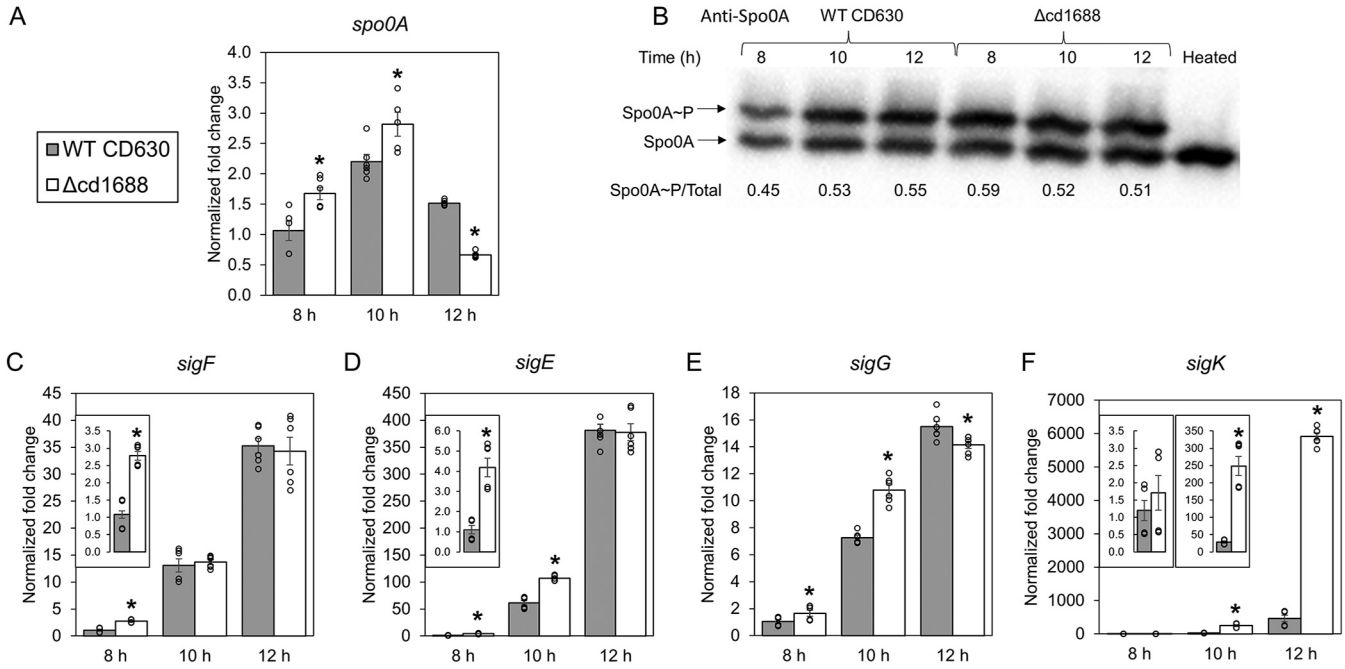

FIG 5 Gene expression profile of sporulation-specific genes and levels of phosphorylated Spo0A in *C. difficile* WT versus the *C. difficile* Δcd1688 strain. (A) Transcript abundance of *spo0A* in the Δcd1688 strain at 8 h, 10 h, and 12 h postinoculation on 70:30 medium relative to the WT sample at 8 h. (B) Detection of Spo0A phosphorylation. Cell lysates isolated from *C. difficile* WT and Δcd1688 strains at 8 h, 10 h, and 12 h postinoculation on 70:30 sporulation agar were resolved via Phos-tag SDS-PAGE and subjected to immunoblotting using anti-Spo0A antibody. (C to F) Transcript abundance of *sigF* (C), *sigE* (D), *sigG* (E), and *sigK* (F). All gene expression was measured via qRT-PCR from RNA samples isolated at 8 h, 10 h, and 12 h postinoculation on 70:30 sporulation media. *, $P \leq 0.05$ as determined by Student's *t* test compared to the *C. difficile* WT630 strain at the same time point.

to initiate cleavage of pro-SigE into mature SigE (19, 49, 50). A previous study in *C. difficile* confirmed that no processing of pro-SigE occurred in a *spoIIR* deletion strain and cells were arrested at the asymmetric division stage (48). We had observed an increase in expression of *spoIIR* (*cd3564*) during growth in BHIS in the *C. difficile* Δcd1688 strain (Fig. 2). Thus, we also tested expression of *spoIIR* during growth on 70:30 sporulation plates. Expression of *spoIIR* was increased 4.7-fold, 1.8-fold, and 1.3-fold in the *C. difficile* Δcd1688 strain at 8 h,10 h, and 12 h, respectively, postinoculation on 70:30 sporulation media (Fig. 6A).

Since *spoIIR* was predicted to contain a CD1688 binding site in the upstream region, we aimed to determine if this RR directly binds to the promoter region of *spoIIR* or if the changes were only due to the observed changes in *sigF* and *spo0A* expression. We performed electrophoretic mobility shift assays (EMSAs) between purified CD1586 (100% identical homolog of CD1688 in strain CDR20291, produced and purified for our previous study [31]) and the *spoIIR* promoter region. CD1586 was shown to cause a gel shift when incubated with the *spoIIR* promoter region, confirming a direct interaction *in vitro* (Fig. 6B and Fig. S6A). No gel shift was observed between CD1586/1688 and a negative-control oligonucleotide, which contained a permuted binding motif (Fig. S6B).

Deletion of *cd1688* results in increased processing of SigE at an earlier time point. Based on the previous results and the dependence of SigE processing on SpoIIR (48), we hypothesized that the increased expression of *spoIIR* may lead to a greater amount of mature SigE in the *C. difficile* Δcd1688 strain than the WT. We performed Western blot analysis on cell lysates at 8 h, 10 h, and 12 h postinoculation on 70:30 sporulation plates using an anti-SigE antibody. Significantly higher total amounts of SigE were observed at the 8-h and 10-h time points in the *C. difficile* Δcd1688 strain than the WT strain (Fig. 6C and D), which was consistent with the gene expression data (Fig. 5D). Additionally, at 8 h, there was a higher ratio of mature SigE to pro-SigE in the *C. difficile* Δcd1688 strain than the WT strain (Fig. 6C and E).

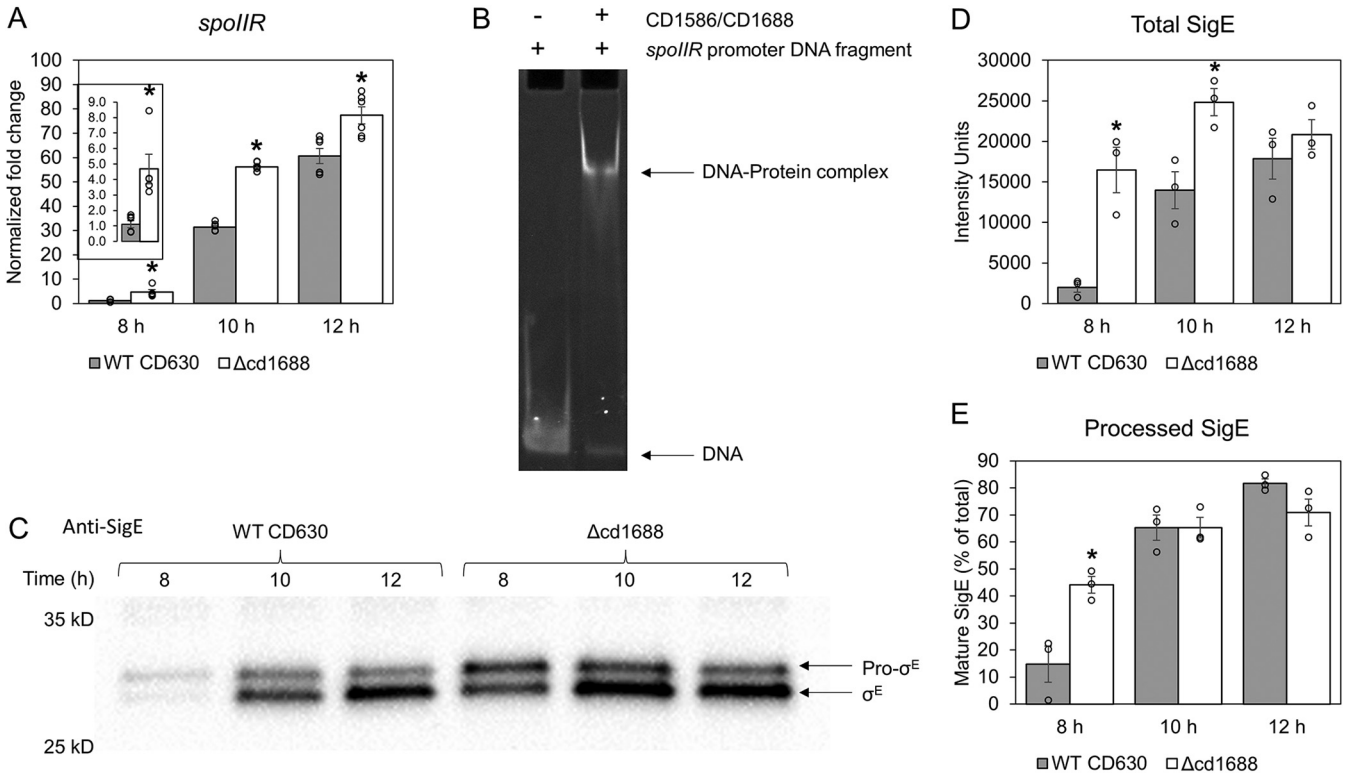

FIG 6 Altered expression of *spoIIR* and SpoIIR-dependent processing of SigE in *C. difficile* Δcd1688. (A) Transcript abundance of *spoIIR* in the *C. difficile* Δcd1688 strain at 8 h, 10 h, and 12 h postinoculation on 70:30 sporulation media measured via qRT-PCR relative to the WT strain 8 h sample. *, $P \leq 0.05$. (B) EMSA analysis indicating *in vitro* binding between RR CD1586/CD1688 and the *spoIIR* promoter region. (C) Western blot analysis of cell lysates isolated from the *C. difficile* WT and Δcd1688 strains at 8 h, 10 h, and 12 h postinoculation on 70:30 sporulation agar. A total of 15 μg of protein was resolved by SDS-PAGE and subjected to immunoblotting using anti-SigE antibody. (D) The amount of total SigE (pro- and mature forms) was determined by quantification of band intensities in the immunoblot using ImageJ. (E) Percentage of processed, mature SigE. The intensity of mature SigE was divided by total intensity of SigE (pro-SigE plus mature SigE) in each sample.

Given that the sporulation pathway involves a hierarchical cascade of regulatory events, it is difficult to differentiate the effect of the increase in expression of *spo0A* versus *spoIIR* in the Δcd1688 strain. Spo0A controls the expression of *sigE* and *sigF*. In turn, it is predicted that both Spo0A and SigF control the expression of *spoIIR*. Therefore, we also checked the protein levels of Spo0A and SigF via Western blot analysis at the earliest time point (8 h). SigF was significantly increased in the Δcd1688 strain compared to WT (Fig. S7A). Spo0A was also slightly increased in the Δcd1688 strain, but this change was not statistically significant (Fig. S7B).

Phosphorylation of CD1688 is necessary for the repression of sporulation in *C. difficile*. Typically, phosphotransfer in TCSs occurs between a histidine residue on the HK and an aspartate residue on the RR, and phosphorylation of the RR changes its activity (27). To determine the role of phosphorylation on the activity of CD1688, we constructed a second complement strain harboring a vector with a xylose-inducible promoter driving the expression of *cd1688* containing a single amino acid change of the active site residue from an aspartate (D50) to an alanine (*C. difficile* Δcd1688::p1688^{D50A}), which results in a protein that is unable to be phosphorylated. To evaluate if the hypersporulation phenotype was dependent on the phosphorylation state of CD1688, we compared the sporulation efficiency of the *C. difficile* Δcd1688::p1688^{D50A} complement strain to *C. difficile* Δcd1688, Δcd1688::p1688, and WT strains. The *C. difficile* Δcd1688::1688^{D50A} complement strain had a similar sporulation efficiency to the *C. difficile* Δcd1688 strain (Fig. 3D). These spores were viable at levels similar to *C. difficile* Δcd1688 as measured by ethanol resistance assays (Fig. 3D and Fig. S3). This demonstrated that the restoration to WT sporulation efficiency observed for the *C. difficile* Δcd1688::p1688 complement strain was dependent on phosphorylation of CD1688.

In order to determine if the binding affinity changed between a nonphosphorylatable CD1586/CD1688 and the *spoIIR* promoter, we performed an EMSA with purified CD1586^{D50G}, which had been constructed in our previous work (31). We observed the same gel shift pattern that we had with the WT CD1586 (Fig. S6C), indicating that binding can occur when the RR is not phosphorylated.

DISCUSSION

The ability to produce spores is an essential component of *C. difficile* transmissibility and persistence. The sporulation pathway has been extensively studied in *B. subtilis* (18, 51), and although the overall developmental steps are generally conserved in *C. difficile*, several key regulatory proteins necessary for sporulation initiation are missing in *C. difficile* (10, 17). Previous studies have established a strong link between certain environmental conditions, including pH and nutrient levels, and sporulation efficiency (23, 24, 26, 37, 52, 53). However, the exact regulatory events that lead to sporulation initiation in *C. difficile* remain unknown. Here, we determined the cellular role of CD1688, a response regulator that had been previously implicated in a transposon mutagenesis study to be important in sporulation (32). Taken together, our data demonstrated that CD1688 is a novel negative regulator of sporulation in *C. difficile*.

Previous work in our lab identified the DNA binding motif of RR CD1586/CD1688 and numerous putative gene targets, including several involved in ABC/ion transport, proteolysis, and sporulation (31). Upon deletion of *cd1688*, we observed a significant increase in the majority of these targets, indicating that CD1688 negatively regulates their expression. Furthermore, sporulation efficiency assays demonstrated that upon deletion of *cd1688*, a more than 3-fold increase in sporulation was observed. Sporulation was restored to WT levels when *cd1688* was complemented back into the cells. However, complementation with a nonphosphorylatable CD1688 failed to restore WT sporulation levels, confirming phosphorylation is necessary for repression of sporulation via CD1688. It does not appear that CD1688 acts as a global regulator since the *C. difficile* Δcd1688 strain exhibited no changes in toxin expression or motility. Moreover, a previous study indicated that the loss of *cd1688* also did not affect the ability of *C. difficile* to produce biofilms (54). To note, the Dembek et al. study (32), which initially predicted a role of CD1586 in R20291 sporulation, found that an insertion in this gene resulted in a decrease in spore formation, the opposite effect that we found. Given the high number of genes identified to be associated with sporulation (798) in that study, this may be due to a high degree of variability related to the spore purification methods used in the study that likely resulted in many false positives.

The initiation of sporulation in all characterized spore-forming bacteria is dependent on phosphorylation of the master regulator Spo0A (55, 56). Several global transcriptional regulators are known to modulate the expression of *spo0A* and, thus, entry into sporulation. Both CcpA and CodY negatively influence the expression of *spo0A* in response to carbon availability and BCAAs/GTP, respectively (24, 37, 38). One mechanism by which CcpA and CodY affect sporulation is through the direct regulation of *sinRR′* expression (25). SinRR′ has been shown to influence sporulation, toxin production, and motility in *C. difficile* (41). However, the exact mechanism of this regulation remains unclear. In a previous study, the overexpression of *sinR* resulted in an increase of sporulation, while the overexpression of *sinR′* had the opposite effect (25), further demonstrating the antagonistic relationship between these two proteins. Interestingly, overexpression of the entire *sinRR′* operon also led to an increase in sporulation (25). In our *C. difficile* Δcd1688 strain, we only observed minor changes in the expression of *ccpA* or *codY*. However, we observed a significant increase in the transcript abundance of *sinR* and, to an even greater extent, of *sinR′* in the *C. difficile* Δcd1688 strain compared to WT when grown on sporulation plates. We suspect this change in expression was not a direct gene regulation due to the absence of a predicted CD1688 binding motif in the promoter region of *sinRR′*. However, the hypersporulation phenotype observed for *C. difficile* Δcd1688 may, at least in part, be due to the increase in *sinRR′*.

Further work will be necessary to fully understand the relationship between CD1688 and the expression of the *sin* locus.

It is evident that the expression of several of the genes that encode sporulation-specific regulators was increased in the absence of *cd1688*. We observed a modest increase in the expression of *spo0A* at 8 h (1.7-fold) and 10 h (1.3-fold) postinoculation on sporulation media in the *C. difficile* Δcd1688 strain. However, by the 12-h time point, transcript levels had decreased to below WT levels. We also observed an increase in Spo0A~P at 8 h in the *C. difficile* Δcd1688 strain, which corresponded to an increase in the expression of the Spo0A~P-dependent targets *sigF* (at 8 h) and *sigE* (at 8 h and 10 h). Overall, the genes necessary for sporulation appear to be expressed earlier in the *C. difficile* Δcd1688 strain compared to the WT strain.

The activity of SpoIIR is essential in the sporulation process of *C. difficile* given that a *spoIIR* knockout strain failed to proceed beyond asymmetric division (48). The expression of *spoIIR* in *B. subtilis* is dependent on SigF and ensures the sequential and temporal expression of the distinct transcriptional programs that occur in the mother cell and forespore (57, 58). Once SpoIIR is produced in the forespore, it is secreted into the inner membrane space, where it signals SpoIIGA to cleave pro-SigE into active SigE in the mother cell (49, 50). This relationship is not as tightly coupled in *C. difficile*, given that *spoIIR* expression can occur independently of SigF, likely through Spo0A~P (48). However, SpoIIR is still required for pro-SigE processing and, thus, the continuation of transcription of sporulation genes in the mother cell. The promoter region upstream of *spoIIR* was predicted to contain a CD1688 binding motif (31). The expression of *spoIIR* was increased in the *C. difficile* Δcd1688 strain at all time points measured postinoculation on 70:30 sporulation plates, suggesting that CD1688 typically negatively regulates *spoIIR*. We further confirmed that RR CD1586/CD1688 has the ability to directly bind to the *spoIIR* promoter via EMSA analysis. We hypothesized that the increase in *spoIIR* expression in the *C. difficile* Δcd1688 strain could lead to an increase in pro-SigE processing in the Δcd1688 strain compared to WT, which was confirmed via Western blot analysis. The total amount of SigE protein was higher in the *C. difficile* Δcd1688 strain during growth on sporulation media, and the ratio of mature SigE to pro-SigE was also significantly higher at the 8-h time point. We considered that a possible mechanism contributing to the hypersporulation phenotype of the *C. difficile* Δcd1688 strain could be through this derepression of *spoIIR* in our mutant. We did not observe any difference in binding between a nonphosphorylatable mutant of CD1586/1688 and the *spoIIR* promoter compared to the WT protein *in vitro*. Even though the binding was not affected, we have not yet determined how the cellular activity of CD1688 changes upon phosphorylation. The derepression we observed for *spoIIR* in the Δcd1688 strain could be contributing to the speed in which the sporulation pathway progresses in this mutant. Our future work will focus on deciphering the individual contributions of the increased expression of *spo0A* versus *spoIIR* to the hypersporulation phenotype of the Δcd1688 strain.

In summary, our study shows that CD1688 plays an important regulatory role in the sporulation pathway in *C. difficile*. CD1688 is the first-described transcriptional regulator that directly binds to the promoter region of *spoIIR* and may represent an additional checkpoint in the sporulation pathway. Collectively, our findings suggest that a yet-to-be-determined environmental signal activates the TCS via autophosphorylation of HK CD1689, followed by subsequent phosphoryl transfer to CD1688, which results in repression of sporulation (Fig. 7). Given that several of the other predicted targets of CD1688 encode ABC and ion transporters, future work will focus on determining if there is a nutritional link to this regulation, similar to what has been observed for several other sporulation regulators in *C. difficile* (24, 37, 38). Future studies evaluating the role of the other predicted CD1688 gene targets in sporulation, the effect of phosphorylation on its ability to bind certain promoters, and the identification of the external stimuli sensed by the HK CD1689 will also add to our mechanistic understanding of

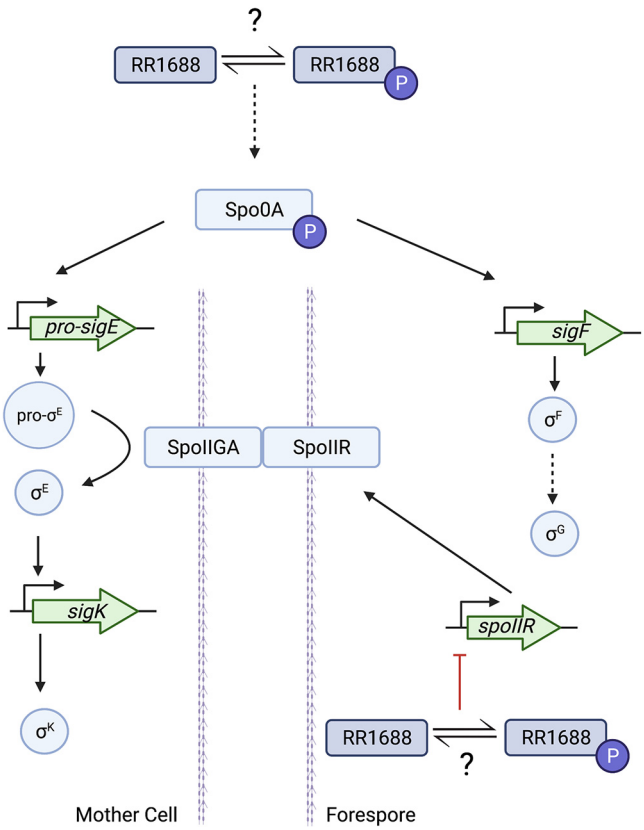

FIG 7 Working model of regulation of sporulation by CD1688. Green arrows represent genes, blue rectangles or circles represent proteins, solid lines indicate known interactions, dashed lines indicate indirect regulation, and red line indicates our proposed regulation via CD1688. Sporulation genes are grouped by their cellular location (either mother cell or forespore). We do not have any evidence that CD1688 is specific to any cellular compartment. Purple circle represents protein phosphorylation. Figure was created using BioRender.com.

spore development in *C. difficile* and will perhaps reveal new gene targets for therapeutic development.

MATERIALS AND METHODS

Bacterial cultivation. The bacterial strains and plasmids used in this study are listed in Table S1 in the supplemental material. *C. difficile* 630 strains were routinely cultured in brain heart infusion (Sigma-Aldrich) medium supplemented with yeast extract (BHIS) containing appropriate antibiotics (2-10 μg/mL thiamphenicol, 250 μg/mL D-cycloserine, or 8 μg/mL cefoxitin) or in 70:30 sporulation medium that contained 70% SMC (90 g Bacto peptone, 5 g protease peptone, 1 g ammonium sulfate, 1.5 g Tris base, and 15 g agar per L) and 30% BHIS (59). Taurocholate (TA) was added to a final concentration of 0.1%, where indicated, as a germinant. To induce expression of *cd1688* in the complement strains, 0.1% xylose was added to growth media where indicated. *C. difficile* was cultured in an anaerobic chamber (Coy Laboratory Products) at 37°C with an atmosphere of 3.5% H_2 and 5 to 8% CO_2 and balanced with N_2 (60). *Escherichia coli* strains were grown at 37°C in Luria-Bertani media (LB) with antibiotics as necessary (20 μg/mL chloramphenicol or 50 μg/mL kanamycin).

Strain and plasmid construction. The CRISPR-Cas9 nickase vector used for generating the mutant strain was constructed using pTMS001 as a backbone as described previously (33). Briefly, three elements were assembled into the backbone, the left homology arm, the right homology arm, and a custom guide RNA (gRNA) designed to target *cd1688*. These regions were PCR amplified from CD630 genomic DNA (gDNA) using Q5 high-fidelity DNA polymerase (NEB) or synthesized by Integrated DNA Technologies (IDT) as a gBlock (oligonucleotides are listed in Table S2). The backbone was linearized via PCR using primers (Pr484 and Pr485) and treated with DpnI following the manufacturer's protocol (NEB) to remove any remaining plasmid template. All fragments (right and left homology arms, linearized backbone, and gRNA) were assembled using HiFi Assembly master mix (NEB) following the manufacturer's protocol, generating the deletion vector (pTMS011).

To complement the *cd1688* deletion, the coding sequence of *cd1688* was PCR amplified using primers BAL36F and BAL36R and cloned into SacI/BamHI-digested pAP114, generating pTMS012, which resulted in the expression of *cd1688* being driven by a xylose-inducible promoter. pAP114 was a gift from Craig Ellermeier and David S. Weiss (Addgene plasmid number 120799) (35). The Q5 site-directed

mutagenesis kit (NEB) was used with primers BAL38F and BAL38R to modify the complement vector pTMS012 to contain an aspartate-to-alanine mutation at amino acid 50, generating pTMS013. Vectors were transferred into DH5α or NEB 10-β cells via transformation, plated on LB with chloramphenicol, and sequence verified (Oklahoma Medical Research Foundation).

Conjugation. Plasmids were transferred into the conjugal donor strain *E. coli* CA434 via electroporation and then into CD630 by conjugation as previously described (61). To generate the *C. difficile* Δcd1688 mutant, several clones were selected and further transferred 3 to 5 times sequentially in BHIS with thiamphenicol. Clones were screened via PCR to confirm loss of *cd1688*, and Sanger sequencing further confirmed the desired mutation was present. Strains were passaged several times in nonselective BHIS to cure the plasmid.

RNA extraction, cDNA synthesis, and qRT-PCR. Overnight *C. difficile* cultures were diluted in fresh BHIS medium to an optical density at 600 nm (OD_{600}) of 0.05 and grown to either exponential (OD_{600}, ~0.5) or stationary growth phase (OD_{600}, ~1.0). Cell pellets were resuspended in TRIzol (Thermo Fisher). Cells grown on 70:30 sporulation agar were scraped from plates at the specified time points, washed with phosphate-buffered saline (PBS), and resuspended in TRIzol. RNA was extracted using the Direct-zol RNA MiniPrep Plus kit following the manufacturer's protocol (Zymo Research). Samples were treated with Turbo DNase I to remove contaminating gDNA, following the manufacturer's protocol (Thermo Fisher). cDNA was synthesized from 1 μg of total RNA using LunaScript RT supermix (NEB). Samples containing no reverse transcriptase enzyme were used as the template in subsequent qPCRs to ensure no gDNA contamination was present. qRT-PCR analysis was performed in technical triplicate with 25 ng cDNA per reaction mixture using LunaScript qPCR master mix (NEB). Samples were normalized to the housekeeping gene *rpoC* and/or *rpoB*, and differences in gene expression were calculated using the Pfaffl comparative method (62). The normalized fold change was calculated for expression of each gene in the Δcd1688 strain relative to expression in the WT630 strain in the same growth conditions or at the 8-h time point as indicated in the figure legends. Efficiencies of the primers were analyzed using serial dilutions of cDNA. Primers are listed in Table S2. We performed three technical replicates for three biological replicates and presented the mean along with the standard error of the mean. Statistical significance was calculated using two-tailed Student's *t* test. All statistical tests were performed in R version 4.1.2 (63).

Sporulation assays. Sporulation efficiency determination and microscopy imaging were performed as described previously (34, 52, 64). *C. difficile* cultures were grown overnight in BHIS-TA and then back diluted in fresh BHIS-TA to an OD_{600} of 0.05. Once the cultures reached an OD_{600} of 0.5, 150 μL was spread on prereduced 70:30 sporulation plates. Cells/spores were harvested at the specified time points. For microscopy (phase contrast), cells were scraped from plates, resuspended in PBS, and removed from the anaerobic chamber. Cells were pelleted and resuspended in 1 mL of PBS. A small volume (5 to 8 μL) of the resuspended culture was applied to a 0.7% agarose pad, covered with a cover slip, and imaged via phase-contrast microscopy using an Olympus BX51 microscope. At least three fields were obtained per strain, and vegetative cells and spores were counted. For ethanol resistance assays, cells were scraped from 70:30 sporulation plates after 24 h growth and resuspended in 5 mL of BHIS to an OD_{600} of 1.0. Serial dilutions were performed and plated onto BHIS agar plates to enumerate vegetative cells. A 0.5-mL aliquot of the cell mixture was mixed with 0.2 mL of distilled water (dH_2O) and 0.3 mL of 95% ethanol (final concentration, 28.5% ethanol) and incubated for 15 min at room temperature. The sample was then serially diluted and plated on BHIS-TA plates to enumerate ethanol-resistant spores. The percent sporulation efficiency was calculated as $\frac{\text{number of EtOH} - \text{resistant spores}}{\text{number of vegetative cells} + \text{number of EtOH} - \text{resistant spores}} \times 100$.

Three biological replicates were performed, and the standard error of the mean was calculated. A one-way analysis of variance (ANOVA) followed by Dunnett's multiple-comparison test was performed to measure statistical significance compared to the WT strain.

Western blot analysis. Cultures of *C. difficile* were grown overnight in BHIS-TA and then back diluted to an OD_{600} of 0.05 using fresh BHIS-TA and grown to an OD_{600} of 0.5. Aliquots of 150 μL were then spread onto 70:30 sporulation plates, grown for the indicated times at 37°C, and collected as described above. Cell pellets were resuspended in 2% SDS containing 4 M urea and lysed using bead beating. Samples were diluted, and protein concentrations were determined using the Pierce bicinchoninic acid (BCA) protein assay kit (Thermo Fisher).

Total protein samples (15 μg) were resolved on a 12% SDS-PAGE gel and transferred to a nitrocellulose membrane. The membrane was blocked using 1% milk in TBST (Tris-buffered saline with 0.1% Tween 20) and probed with the specified primary antibody (diluted 1:2,000) overnight at 4°C, followed by washing with TBST and incubation with horseradish peroxidase (HRP)-conjugated secondary antibody (diluted 1:3,000; Sigma) for 30 min at room temperature. Primary antibodies were a generous gift from Aimee Shen (Tufts University). The blots were developed using the Bio-Rad Clarity Western ECL kit, and proteins were visualized using a ChemiDoc MP charge-coupled-device (CCD) imaging system. Densitometry was performed using ImageJ. Western blotting was performed for three biological replicates, and a representative blot is presented.

Phos-tag gel Western blotting was performed as described below. Gels were prepared according to the manufacturer's instructions (Fujifilm Wako Chemicals Inc., USA), and 12% SDS-PAGE gels were copolymerized with 50 μM Phos-tag acrylamide and 10 μM $MnCl_2$. Total protein lysates (10 μg) were resolved by electrophoresis and then electroblotted to a nitrocellulose membrane. Western blots were performed as described above except the primary Spo0A antibody was diluted 1:1,000. To confirm that the slower-migrating bands represented phosphorylated proteins, duplicate samples were heated at 95°C for 5 min to hydrolyze the phosphoryl group prior to loading on the gel.

EMSA. EMSAs of CD1586 or a nonphosphorylatable mutant ($CD1586^{D50G}$) and DNA were run as previously described (31). Briefly, pairs of single-stranded oligonucleotides (Table S2) were annealed at 95°C

for 5 min in 10 mM Tris, pH 8.0, and 50 mM NaCl. Samples were cooled to room temperature. Protein (concentration as indicated) and double-stranded DNA (dsDNA; 0.5 μM) were incubated at room temperature for 10 min in binding buffer (10 mM Tris, pH 8.0, 50 mM NaCl, and 10 mM $MgCl_2$). Samples were separated on a prerun 10% polyacrylamide gel and run at 120 V for 1 h, submerged in ice. DNA was stained using 0.5× TBE containing ethidium bromide for 5 min. Images were captured using a Gel Logic 100 system with a UV transilluminator.

SUPPLEMENTAL MATERIAL

Supplemental material is available online only.

SUPPLEMENTAL FILE 1, PDF file, 0.9 MB.

ACKNOWLEDGMENTS

We are grateful to Fabiola Janiak-Spens and Kriti Shukla for their helpful discussions during the project and their valuable contribution to manuscript editing. We thank Elizabeth Karr for access to an anaerobic chamber and Aimee Shen for the generous gift of primary antibodies.

Funding for the project was provided by the Oklahoma Center for the Advancement of Science and Technology (HR18-110 to A.H.W.), Grayce B. Kerr Endowment funds (to A.H.W.), the Price Family Foundation (to A.H.W.), National Institutes of Health grant number R01AI119048 (to J.D.B.), and a Cottrell Postdoctoral Fellowship from Research Corporation for Science Advancement (to M.L.K.). The OU Protein Production and Characterization Core (PPCC) facility is supported by an Institutional Development Award (IDeA) from the National Institute of General Medical Sciences of the National Institutes of Health under grant number P20GM103640.

REFERENCES

1. Centers for Disease Control and Prevention. 2019. Antibiotic resistance threats in the United States, 2019. U.S. Department of Health and Human Services, Centers for Disease Control and Prevention, Atlanta, GA.
2. George RH, Symonds JM, Dimock F, Brown JD, Arabi Y, Shinagawa N, Keighley MR, Alexander-Williams J, Burdon DW. 1978. Identification of *Clostridium difficile* as a cause of pseudomembranous colitis. Br Med J 1:695. https://doi.org/10.1136/bmj.1.6114.695.
3. Zhu D, Sorg JA, Sun X. 2018. *Clostridioides difficile* biology: sporulation, germination, and corresponding therapies for *C. difficile* infection. Front Cell Infect Microbiol 8:29. https://doi.org/10.3389/fcimb.2018.00029.
4. Barbut F, Richard A, Hamadi K, Chomette V, Burghoffer B, Petit J-C. 2000. Epidemiology of recurrences or reinfections of *Clostridium difficile*-associated diarrhea. J Clin Microbiol 38:2386–2388. https://doi.org/10.1128/JCM.38.6.2386-2388.2000.
5. Lawley TD, Croucher NJ, Yu L, Clare S, Sebaihia M, Goulding D, Pickard DJ, Parkhill J, Choudhary J, Dougan G. 2009. Proteomic and genomic characterization of highly infectious *Clostridium difficile* 630 spores. J Bacteriol 191:5377–5386. https://doi.org/10.1128/JB.00597-09.
6. Dawson LF, Valiente E, Donahue EH, Birchenough G, Wren BW. 2011. Hypervirulent *Clostridium difficile* PCR-ribotypes exhibit resistance to widely used disinfectants. PLoS One 6:e25754. https://doi.org/10.1371/journal.pone.0025754.
7. Lawley TD, Clare S, Deakin LJ, Goulding D, Yen JL, Raisen C, Brandt C, Lovell J, Cooke F, Clark TG, Dougan G. 2010. Use of purified *Clostridium difficile* spores to facilitate evaluation of health care disinfection regimens. Appl Environ Microbiol 76:6895–6900. https://doi.org/10.1128/AEM.00718-10.
8. Gerding Dale N, Muto Carlene A, Owens J, Robert C. 2008. Measures to control and prevent *Clostridium difficile* infection. Clin Infect Dis 46:S43–S49. https://doi.org/10.1086/521861.
9. Shen A, Edwards AN, Sarker MR, Paredes-Sabja D. 2019. Sporulation and germination in clostridial pathogens. Microbiol Spectr 7. https://doi.org/10.1128/microbiolspec.GPP3-0017-2018.
10. Underwood S, Guan S, Vijayasubhash V, Baines SD, Graham L, Lewis RJ, Wilcox MH, Stephenson K. 2009. Characterization of the sporulation initiation pathway of *Clostridium difficile* and its role in toxin production. J Bacteriol 191:7296–7305. https://doi.org/10.1128/JB.00882-09.
11. Edwards AN, McBride SM. 2014. Initiation of sporulation in *Clostridium difficile*: a twist on the classic model. FEMS Microbiol Lett 358:110–118. https://doi.org/10.1111/1574-6968.12499.
12. Pettit LJ, Browne HP, Yu L, Smits W, Fagan RP, Barquist L, Martin MJ, Goulding D, Duncan SH, Flint HJ, Dougan G, Choudhary JS, Lawley TD. 2014. Functional genomics reveals that *Clostridium difficile* Spo0A coordinates sporulation, virulence and metabolism. BMC Genomics 15:160. https://doi.org/10.1186/1471-2164-15-160.
13. Fimlaid KA, Bond JP, Schutz KC, Putnam EE, Leung JM, Lawley TD, Shen A. 2013. Global analysis of the sporulation pathway of *Clostridium difficile*. PLoS Genet 9:e1003660. https://doi.org/10.1371/journal.pgen.1003660.
14. Rosenbusch KE, Bakker D, Kuijper EJ, Smits WK. 2012. C. difficile 630Δerm Spo0A regulates sporulation, but does not contribute to toxin production, by direct high-affinity binding to target DNA. PLoS One 7:e48608. https://doi.org/10.1371/journal.pone.0048608.
15. Sonenshein AL. 2000. Control of sporulation initiation in *Bacillus subtilis*. Curr Opin Microbiol 3:561–566. https://doi.org/10.1016/s1369-5274(00)00141-7.
16. Pereira FC, Saujet L, Tomé AR, Serrano M, Monot M, Couture-Tosi E, Martin-Verstraete I, Dupuy B, Henriques AO. 2013. The spore differentiation pathway in the enteric pathogen *Clostridium difficile*. PLoS Genet 9:e1003782. https://doi.org/10.1371/journal.pgen.1003782.
17. Paredes CJ, Alsaker KV, Papoutsakis ET. 2005. A comparative genomic view of clostridial sporulation and physiology. Nat Rev Microbiol 3:969–978. https://doi.org/10.1038/nrmicro1288.
18. Burbulys D, Trach KA, Hoch JA. 1991. Initiation of sporulation in *B. subtilis* is controlled by a multicomponent phosphorelay. Cell 64:545–552. https://doi.org/10.1016/0092-8674(91)90238-T.
19. Higgins D, Dworkin J. 2012. Recent progress in *Bacillus subtilis* sporulation. FEMS Microbiol Rev 36:131–148. https://doi.org/10.1111/j.1574-6976.2011.00310.x.
20. Childress KO, Edwards AN, Nawrocki KL, Anderson SE, Woods EC, McBride SM. 2016. The phosphotransfer protein CD1492 represses sporulation initiation in *Clostridium difficile*. Infect Immun 84:3434–3444. https://doi.org/10.1128/IAI.00735-16.
21. Lee C, Rizvi A, Edwards AN, DiCandia MA, Vargas Cuebas G, Monteiro M, McBride SM. 2022. Genetic mechanisms governing sporulation initiation in *Clostridioides difficile*. Curr Opin Microbiol 66:32–38. https://doi.org/10.1016/j.mib.2021.12.001.
22. Edwards AN, Wetzel D, DiCandia MA, McBride SM. 2022. Three orphan histidine kinases inhibit Clostridioides difficile sporulation. J Bacteriol 204:e0010622. https://doi.org/10.1128/jb.00106-22.

23. Nawrocki KL, Edwards AN, Daou N, Bouillaut L, McBride SM. 2016. CodY-dependent regulation of sporulation in *Clostridium difficile*. J Bacteriol 198:2113–2130. https://doi.org/10.1128/JB.00220-16.
24. Antunes A, Camiade E, Monot M, Courtois E, Barbut F, Sernova NV, Rodionov DA, Martin-Verstraete I, Dupuy B. 2012. Global transcriptional control by glucose and carbon regulator CcpA in *Clostridium difficile*. Nucleic Acids Res 40:10701–10718. https://doi.org/10.1093/nar/gks864.
25. Girinathan BP, Ou J, Dupuy B, Govind R. 2018. Pleiotropic roles of *Clostridium difficile sin* locus. PLoS Pathog 14:e1006940. https://doi.org/10.1371/journal.ppat.1006940.
26. Martins D, DiCandia MA, Mendes AL, Wetzel D, McBride SM, Henriques AO, Serrano M. 2021. CD25890, a conserved protein that modulates sporulation initiation in *Clostridioides difficile*. Sci Rep 11:7887. https://doi.org/10.1038/s41598-021-86878-9.
27. West AH, Stock AM. 2001. Histidine kinases and response regulator proteins in two-component signaling systems. Trends Biochem Sci 26:369–376. https://doi.org/10.1016/s0968-0004(01)01852-7.
28. Bourret RB. 2010. Receiver domain structure and function in response regulator proteins. Curr Opin Microbiol 13:142–149. https://doi.org/10.1016/j.mib.2010.01.015.
29. Galperin MY. 2010. Diversity of structure and function of response regulator output domains. Curr Opin Microbiol 13:150–159. https://doi.org/10.1016/j.mib.2010.01.005.
30. Zschiedrich CP, Keidel V, Szurmant H. 2016. Molecular mechanisms of two-component signal transduction. J Mol Biol 428:3752–3775. https://doi.org/10.1016/j.jmb.2016.08.003.
31. Hebdon SD, Menon SK, Richter-Addo GB, Karr EA, West AH. 2018. Regulatory targets of the response regulator RR_1586 from *Clostridioides difficile* identified using a bacterial one-hybrid screen. J Bacteriol 200:e00351-18. https://doi.org/10.1128/JB.00351-18.
32. Dembek M, Barquist L, Boinett CJ, Cain AK, Mayho M, Lawley TD, Fairweather NF, Fagan RP. 2015. High-throughput analysis of gene essentiality and sporulation in *Clostridium difficile*. mBio 6:e02383. https://doi.org/10.1128/mBio.02383-14.
33. Ahmed UKB, Shadid TM, Larabee JL, Ballard JD. 2020. Combined and distinct roles of Agr proteins in *Clostridioides difficile* 630 sporulation, motility, and toxin production. mBio 11:e03190-20. https://doi.org/10.1128/mBio.03190-20.
34. Shen A, Fimlaid KA, Pishdadian K. 2016. Inducing and quantifying *Clostridium difficile* spore formation. Methods Mol Biol 1476:129–142. https://doi.org/10.1007/978-1-4939-6361-4_10.
35. Müh U, Pannullo AG, Weiss DS, Ellermeier CD. 2019. A xylose-inducible expression system and a CRISPR interference plasmid for targeted knockdown of gene expression in *Clostridioides difficile*. J Bacteriol 201:e00711-18. https://doi.org/10.1128/JB.00711-18.
36. Daou N, Wang Y, Levdikov VM, Nandakumar M, Livny J, Bouillaut L, Blagova E, Zhang K, Belitsky BR, Rhee K, Wilkinson AJ, Sun X, Sonenshein AL. 2019. Impact of CodY protein on metabolism, sporulation and virulence in *Clostridioides difficile* ribotype 027. PLoS One 14:e0206896. https://doi.org/10.1371/journal.pone.0206896.
37. Dineen SS, McBride SM, Sonenshein AL. 2010. Integration of metabolism and virulence by *Clostridium difficile* CodY. J Bacteriol 192:5350–5362. https://doi.org/10.1128/JB.00341-10.
38. Dineen SS, Villapakkam AC, Nordman JT, Sonenshein AL. 2007. Repression of *Clostridium difficile* toxin gene expression by CodY. Mol Microbiol 66:206–219. https://doi.org/10.1111/j.1365-2958.2007.05906.x.
39. Bai U, Mandic-Mulec I, Smith I. 1993. SinI modulates the activity of SinR, a developmental switch protein of *Bacillus subtilis*, by protein-protein interaction. Genes Dev 7:139–148. https://doi.org/10.1101/gad.7.1.139.
40. Mandic-Mulec I, Doukhan L, Smith I. 1995. The *Bacillus subtilis* SinR protein is a repressor of the key sporulation gene *spo0A*. J Bacteriol 177:4619–4627. https://doi.org/10.1128/jb.177.16.4619-4627.1995.
41. Ciftci Y, Girinathan BP, Dhungel BA, Hasan MK, Govind R. 2019. *Clostridioides difficile* SinR' regulates toxin, sporulation and motility through protein-protein interaction with SinR. Anaerobe 59:1–7. https://doi.org/10.1016/j.anaerobe.2019.05.002.
42. Edwards AN, Anjuwon-Foster BR, McBride SM. 2019. RstA is a major regulator of *Clostridioides difficile* toxin production and motility. mBio 10:e01991-18. https://doi.org/10.1128/mBio.01991-18.
43. Edwards AN, Tamayo R, McBride SM. 2016. A novel regulator controls *Clostridium difficile* sporulation, motility and toxin production. Mol Microbiol 100:954–971. https://doi.org/10.1111/mmi.13361.
44. Fimlaid KA, Shen A. 2015. Diverse mechanisms regulate sporulation sigma factor activity in the *Firmicutes*. Curr Opin Microbiol 24:88–95. https://doi.org/10.1016/j.mib.2015.01.006.
45. McBride SM, Sonenshein AL. 2011. Identification of a genetic locus responsible for antimicrobial peptide resistance in *Clostridium difficile*. Infect Immun 79:167–176. https://doi.org/10.1128/IAI.00731-10.
46. Saujet L, Pereira FC, Henriques AO, Martin-Verstraete I. 2014. The regulatory network controlling spore formation in *Clostridium difficile*. FEMS Microbiol Lett 358:1–10. https://doi.org/10.1111/1574-6968.12540.
47. Hilbert DW, Piggot PJ. 2004. Compartmentalization of gene expression during *Bacillus subtilis* spore formation. Microbiol Mol Biol Rev 68:234–262. https://doi.org/10.1128/MMBR.68.2.234-262.2004.
48. Saujet L, Pereira FC, Serrano M, Soutourina O, Monot M, Shelyakin PV, Gelfand MS, Dupuy B, Henriques AO, Martin-Verstraete I. 2013. Genome-wide analysis of cell type-specific gene transcription during spore formation in *Clostridium difficile*. PLoS Genet 9:e1003756. https://doi.org/10.1371/journal.pgen.1003756.
49. Karow ML, Glaser P, Piggot PJ. 1995. Identification of a gene, *spoIIR*, that links the activation of sigma E to the transcriptional activity of sigma F during sporulation in *Bacillus subtilis*. Proc Natl Acad Sci U S A 92:2012–2016. https://doi.org/10.1073/pnas.92.6.2012.
50. Londono-Vallejo JA, Stragier P. 1995. Cell-cell signaling pathway activating a developmental transcription factor in *Bacillus subtilis*. Genes Dev 9:503–508. https://doi.org/10.1101/gad.9.4.503.
51. Hoch JA. 2000. Two-component and phosphorelay signal transduction. Curr Opin Microbiol 3:165–170. https://doi.org/10.1016/S1369-5274(00)00070-9.
52. Edwards AN, Nawrocki KL, McBride SM. 2014. Conserved oligopeptide permeases modulate sporulation initiation in *Clostridium difficile*. Infect Immun 82:4276–4291. https://doi.org/10.1128/IAI.02323-14.
53. Wetzel D, McBride SM. 2020. The impact of pH on *Clostridioides difficile* sporulation and physiology. Appl Environ Microbiol 86:e02706-19. https://doi.org/10.1128/AEM.02706-19.
54. Dubois T, Tremblay YDN, Hamiot A, Martin-Verstraete I, Deschamps J, Monot M, Briandet R, Dupuy B. 2019. A microbiota-generated bile salt induces biofilm formation in *Clostridium difficile*. NPJ Biofilms Microbiomes 5:14. https://doi.org/10.1038/s41522-019-0087-4.
55. Galperin MY, Mekhedov SL, Puigbo P, Smirnov S, Wolf YI, Rigden DJ. 2012. Genomic determinants of sporulation in *Bacilli* and *Clostridia*: towards the minimal set of sporulation-specific genes. Environ Microbiol 14:2870–2890. https://doi.org/10.1111/j.1462-2920.2012.02841.x.
56. Traag BA, Pugliese A, Eisen JA, Losick R. 2013. Gene conservation among endospore-forming bacteria reveals additional sporulation genes in *Bacillus subtilis*. J Bacteriol 195:253–260. https://doi.org/10.1128/JB.01778-12.
57. Steil L, Serrano M, Henriques AO, Volker U. 2005. Genome-wide analysis of temporally regulated and compartment-specific gene expression in sporulating cells of *Bacillus subtilis*. Microbiology (Reading) 151:399–420. https://doi.org/10.1099/mic.0.27493-0.
58. Wang ST, Setlow B, Conlon EM, Lyon JL, Imamura D, Sato T, Setlow P, Losick R, Eichenberger P. 2006. The forespore line of gene expression in *Bacillus subtilis*. J Mol Biol 358:16–37. https://doi.org/10.1016/j.jmb.2006.01.059.
59. Putnam EE, Nock AM, Lawley TD, Shen A. 2013. SpoIVA and SipL are *Clostridium difficile* spore morphogenetic proteins. J Bacteriol 195:1214–1225. https://doi.org/10.1128/JB.02181-12.
60. Edwards AN, Suárez JM, McBride SM. 2013. Culturing and maintaining *Clostridium difficile* in an anaerobic environment. J Vis Exp e50787. https://doi.org/10.3791/50787.
61. Kirk JA, Fagan RP. 2016. Heat shock increases conjugation efficiency in *Clostridium difficile*. Anaerobe 42:1–5. https://doi.org/10.1016/j.anaerobe.2016.06.009.
62. Pfaffl MW. 2001. A new mathematical model for relative quantification in real-time RT-PCR. Nucleic Acids Res 29:e45. https://doi.org/10.1093/nar/29.9.e45.
63. R Core Team. 2021. R: a language and environment for statistical computing. R Foundation for Statistical Computing, Vienna, Austria.
64. Edwards AN, McBride SM. 2016. Isolating and purifying *Clostridium difficile* spores, p 117–128. *In* Roberts AP, Mullany P (ed), *Clostridium difficile*, vol 1476. Springer New York, New York, NY.